Catalysis Today 164 (2011) 181–185

Contents lists available at ScienceDirect

Catalysis Today

journal homepage: www.elsevier.com/locate/cattod

Study of Pt-free anode catalysts for anion exchange membrane fuel cells

Tomokazu Sakamoto*, Koichiro Asazawa, Koji Yamada, Hirohisa Tanaka

Advanced R&D Division, DAIHATSU Motor Co. Ltd., 3000, Yamanoue, Ryuo-cho, Gamo-gun, Shiga 520-2593, Japan

ARTICLE INFO

Article history:
Received 1 July 2010
Received in revised form 2 November 2010
Accepted 2 November 2010
Available online 4 December 2010

Keywords:
Transition metal catalysts
Hydrazine
Precious metal-free liquid feed fuel cells

ABSTRACT

Unsupported transition-metal nanoparticles such as Ni, Co, and Ni_xCo_y ($Ni_{0.75}Co_{0.25}$, $Ni_{0.50}Co_{0.50}$, $Ni_{0.25}Co_{0.75}$) were synthesized by the liquid reduction process for application to the anode catalyst of Precious Metal-free Liquid feed Fuel Cells (PM-fLFCs) using hydrazine hydrate ($N_2H_4{\cdot}H_2O$) for a fuel. Their electrocatalytic activities were evaluated by rotating disk electrode (RDE), and the mass activity of $Ni_{0.50}Co_{0.50}$ exhibited higher activity than other catalysts for the anodic oxidation of hydrazine in alkaline solution. The morphology and structure of these catalysts were characterized by X-ray diffraction (XRD), transmission electron microscopy (TEM), energy dispersive X-ray spectroscopy (EDS), and X-ray photoemission spectroscopy (XPS). It has been indicated that $Ni_{0.50}Co_{0.50}$ has a coexistence effect by inhabitation of Co oxidation and significantly improve the electrooxidation of hydrazine. The excellent fuel cell performance, 0.891 V of open circuit voltage and 432 mW/cm^2 of high maximum power, was exhibited using $Ni_{0.50}Co_{0.50}$ catalysts.

1. Introduction

The direct hydrazine fuel cells were investigated as hydrazine can be considered a green fuel source since it does not produce CO or CO_2 as it is oxidized, which in turn means that hydrazine fuel cells will not suffer from any CO poisoning effects [1–3]. In recent research, PM-fLFCs have been reported that can effectively improve the power density of anionic fuel cells and resolve two barriers of proton exchange membrane fuel cells [4]. One of the remarkable features of PM-fLFCs is the use of liquid hydrazine hydrate for a fuel, which is believed that existing infrastructures can be applied it to refuel and store. Another one is the use of transition metals such as Ni or Co for the anode catalyst, Co or Ag for the cathode catalyst. In an anionic fuel cells, since the solid hydroxide anion (OH^-) exchange polymer membrane is used, it changes to the mild corrosion environment that can use not only Pt but also various kind of metals [5–8].

In most recent research, the binary and ternary transition alloy catalysts supported on the carbon powder were discovered that can significantly oxidize the hydrazine in alkaline media using combinatorial exploration [9]. Asazawa et al. reported the cell performance of unsupported catalysts of commercialized Ni, Co or Pt as the anode catalyst of PM-fLFCs. It was found that Ni or Co showed higher activity than Pt [10]. Thus, it is drawn much attention that Ni and Co compounds enhance the performance of PM-fLFCs drastically.

In this study, unsupported transition metal catalysts such as Ni, Co, and Ni_xCo_y ($Ni_{0.75}Co_{0.25}$, $Ni_{0.50}Co_{0.50}$, and $Ni_{0.25}Co_{0.75}$) have been synthesized using the liquid reduction process for the application to the anode catalyst of PM-fLFCs. The catalytic activity for electrooxidation of hydrazine was performed using RDE and the measurement of cell performance. The morphology and structure of these catalysts were analyzed by XRD, TEM, EDS, and XPS.

2. Experimental

2.1. Catalyst synthesis

Unsupported transition-metal catalysts were carried out using the liquid reduction process without any dispersants. The specified amounts of Ni and Co acetylacetonates (Sigma Aldrich Inc.) as the starting material were dissolved in isopropanol (Hayashi Pure Chemical Ind., Co., Ltd.) by the ultrasonic process for 15 min. The solution was purged by N_2 bubbling for deoxidation. Then, the solution was transferred to a vessel with reflux attachment and placed in a mantle heater and heated to the boiling point at 2.7 °C/min under gentle mechanical stirring at 200 rpm. After keeping at boiling point for 30 min, sodium borohydride (Hayashi Pure Chemical Ind., Co., Ltd.) dissolved in isopropanol was injected to reduce metal precursors. Then the precipitations were recovered from the mother liquor by centrifugal separation, and rinsed with deionized water (Milli-pore Japan Co., Ltd., > 18.2 MΩ). The powder thus obtained was dried at 80 °C in vacuum. To remove organic moieties, the powder was heat-treated at 300 °C for 2 h in a flow of 10% H_2/N_2.

* Corresponding author. Tel.: +81 748 57 1685; fax: +81 748 57 1064.
E-mail address: tomokazu_sakamoto@mail.daihatsu.co.jp (T. Sakamoto).

0920-5861/$ – see front matter.
doi:10.1016/j.cattod.2010.11.012

2.2. Characterization of catalyst

The structure of prepared catalyst was examined using the θ–2θ XRD (Rigaku Corporation, RINT 2000). The Cu Kα source was operating at a potential of 40 kV and a current of 450 mA. 2θ diffraction angles ranged from 10° to 110°. The microstructure was observed by TEM (Hitachi, H-800) with the accelerating voltage of 200 kV. The TEM-EDS (Kevex, 550I) was performed in order to confirm the alloy compositions. The surface of chemical composition was analyzed by XPS (Ulvac Phi Inc., ESCA 5600). The Mg Kα photons ($h\nu$ = 1253.6 eV) were used to excite photoemission. The surfaces of synthesized catalyst were sputtered with an Ar ion beam generated by an ion gun operated at 4.5 kV. The binding energy (BE) scale was calibrated by taking the C 1s peak at 284.6 eV.

2.3. Electrochemical measurement using RDE

Catalyst inks were prepared in a following manner. 10 mg of the catalyst was combined with 1.04 ml of isopropanol, 0.26 ml of THF (Hayashi Pure Chemical Ind., Co., Ltd.) and 0.28 ml of 2 wt.% anionic ionomer solution (Tokuyama Corporation, A3) The ink was then sonicated during 5 min. After sonication, 5 μl of the ink was deposited onto a commercial glassy carbon (GC) electrode (Interchemi Inc., diameter = 5 mm) using a micropipette, resulting in a loading of 0.16 mg/cm^2. The GC electrode deposited ink was then left to dry for at least 30 min in air.

The electrocatalytic activities of the GC electrode deposited a catalyst were examined by a potentiostat (BAS, ALS/600) with RDE (Pine Instrument, AFMSRCE) to perform the electrochemical measurements in 1.0 M KOH (Hayashi Pure Chemical Ind., Co., Ltd.)/0.1 M $N_2H_4{\cdot}H_2O$ (Otsuka Chemical Co., Inc., 60% in H_2O) and to measure the background in 1 M KOH. Prior to measure, GC electrode were polished to a mirror finish with 0.05 μm alumina suspension (BAS Inc.). All measurements were conducted at 60 °C and measured at a speed rotation of 1600 rpm. The LSV during 20 mV/s anodic sweeps is plotted against the applied potential. The electrolytes were bubbled with N_2 for 15 min to remove dissolved O_2 before each measurement. A Pt plate was used as counter electrode and a Hg/HgO (Radiometer Analytical SAS, XR440) immersed in 1.0 M KOH solution was used as a reference electrode. All potentials are reported with respect to a reversible hydrogen electrode (RHE) at pH 14.

2.4. The measurement of cell performance

100 mg of the catalyst was combined with 0.96 ml of isopropanol, 0.24 ml of THF and 0.2 ml of a 5 wt.% anionic ionomer solution. The ink was then sonicated during 5 min. After sonication, the mixture inserted ZrO_2 beads (Nikkato Corporation, diameter = 2.0 mm) were agitated for 15 min. The prepared ink was directly sprayed onto an anionic electrolyte membrane (Tokuyama Corporation, A201). Co-PPY-C (Hokko Chemical Industry Co., Ltd., PPY: polypyrrole) cathode catalyst was formed into an electrode using a similar method to that for the anode. The membrane was then pressed for 5 min at room temperature to bond between catalyst layers and a membrane. The membrane was then immersed in 1.0 M KOH solution for the ion-exchange to OH^- form of an anionic membrane for 8 h.

The prepared MEA, with a round shaped working electrode area of 1 cm^2, was inserted in a single cell to measure the cell performance. The fuel of 1.0 M KOH/1.0 M $N_2H_4{\cdot}H_2O$ was supplied to the anode at flow rate of 2 ml/min, and oxygen gas humidified at 50 °C was supplied to the cathode at the flow rate of 500 ml/min. The applied shape of the flow-fields was serpentine for the anode and comb-shaped for the cathode. The cell temperature was controlled at 80 °C. The operating pressures on both anode and cathode sides were 20 kPa.

3. Results and discussion

XRD spectra of the prepared catalysts from 20° to 100° were shown in Fig. 1. It can be seen that the diffraction peaks at (1 1 1), (2 0 0), (2 2 0), (3 1 1), and (2 2 2) pertain to the face centered cubic (fcc) lattice Ni or Co, and (1 1 1) and (2 2 0) at 2θ = 36.5° and 61.5° pertain to the fcc CoO. The average crystallite sizes of these catalysts were calculated from Ni or Co (1 1 1) according to the Scherrer formula, and summarized in Table 1. The crystallite sizes for these catalysts are smaller than the particle diameter determined from the TEM micrographs. It was suggested that the spherical particles contain a number of small crystals.

The TEM micrographs of as-prepared catalysts (before annealing) and prepared catalysts were shown in Fig. 2(a–f). The diameter of as-prepared catalysts is confirmed approximately 10 nm in Fig. 2(a–c). However particle aggregates are observed in Fig. 2(d–f), and the diameters of prepared catalysts are examined from 20 to 50 nm. The nanoparticles of as-prepared catalysts agglutinated to avoid the use of dispersants, when the powder was annealed in the furnace to remove organic moieties at 300 °C. The electron diffraction patterns (EDPs) in Fig. 2(g–i) correspond to TEM images of prepared catalysts in Fig. 2(d–f). Four fringe patterns with plane distances of 0.204, 0.176, 0.124, and 0.106 nm from inner to outer can be observed in Fig. 2(g). These correspond to the (1 1 1), (2 0 0), (2 2 0), and (3 1 1) diffraction planes of fcc Ni. The same fringe patterns of Fig. 2(g) and amorphous fringe patterns of 0.246, 0.149 nm can be observed in Fig. 2(h and i). These amorphous fringe patterns are corresponded to the (1 1 1), (2 2 0) diffraction plane of

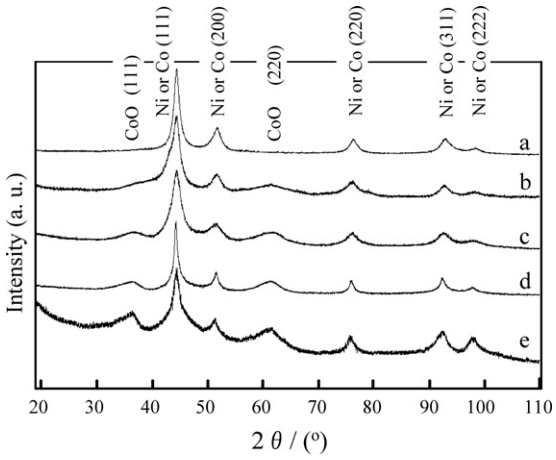

Fig. 1. X-ray diffraction spectra of prepared catalysts of (a) Ni, (b) $Ni_{0.75}Co_{0.25}$, (c) $Ni_{0.50}Co_{0.50}$, (d) $Ni_{0.25}Co_{0.75}$, (e) Co.

Table 1
Typical properties of synthesized Ni, Co, and Ni_xCo_y catalysts.

Catalysts[a]	$Ni(acac)_2$ (mmol)	$Co(acac)_2$ (mmol)	Composition[b] (at.%)	Crystallite size[c] (nm)
Ni	1.00			7.6 ± 0.1
$Ni_{0.75}Co_{0.25}$	0.75	0.25	76:24	3.6 ± 0.1
$Ni_{0.50}Co_{0.50}$	0.50	0.50	53:47	4.1 ± 0.1
$Ni_{0.25}Co_{0.75}$	0.25	0.75	27:73	9.8 ± 0.1
Co		1.00		6.6 ± 0.1

[a] Dissolved in a mixed solvent of isopropanol for the preparation of Ni, Co, and Ni_xCo_y catalysts.
[b] The composition of Ni_xCo_y alloy catalysts was analyzed by EDS.
[c] Average crystallite sizes were calculated from (1 1 1) diffraction peak of Ni or Co in Fig. 1.

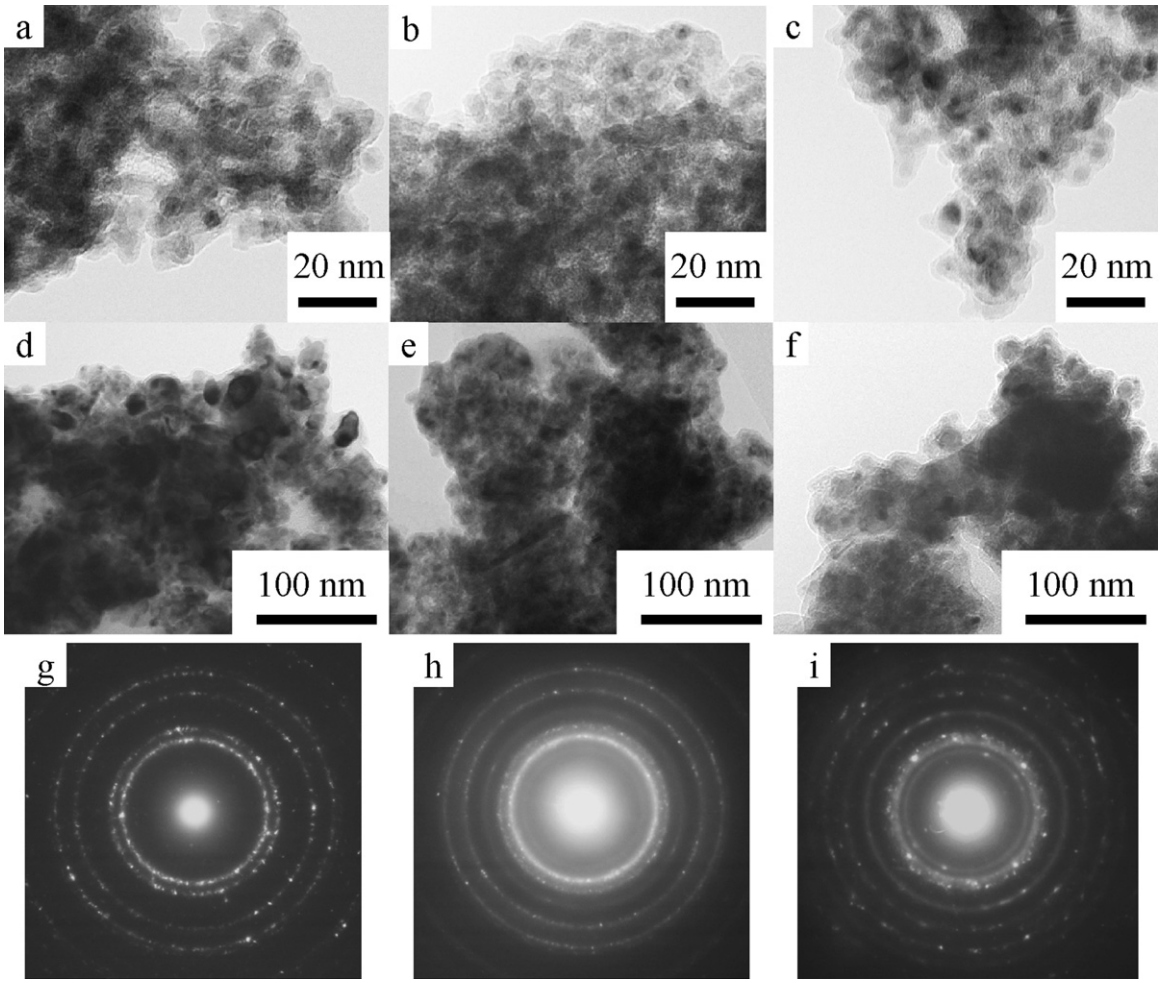

Fig. 2. TEM micrographs of as-prepared catalysts of (a) Ni, (b) $Ni_{0.50}Co_{0.50}$, (c) Co and prepared catalysts of (a) Ni, (b) $Ni_{0.50}Co_{0.50}$, (c) Co. Electron diffraction patterns of prepared catalysts of (a) Ni, (b) $Ni_{0.50}Co_{0.50}$, (c) Co.

fcc CoO. The EDP results well agree with XRD analyses. However, as the plane distance of both fcc Ni and Co is so much close, the discrimination between fcc Ni and Co from XRD and EDP analysis is difficult. Thus, TEM-EDS was used to confirm their phase compositions. Fig. 3 shows TEM-EDS micrographs of the $Ni_{0.50}Co_{0.50}$ alloy catalyst. The both Ni and Co were homogeneously distributed in the prepared catalyst using the liquid reduction process. The $Ni_{0.50}Co_{0.50}$ catalyst was confirmed a solid solution of Ni and Co from TEM-EDS micrographs. The average composition of the alloys

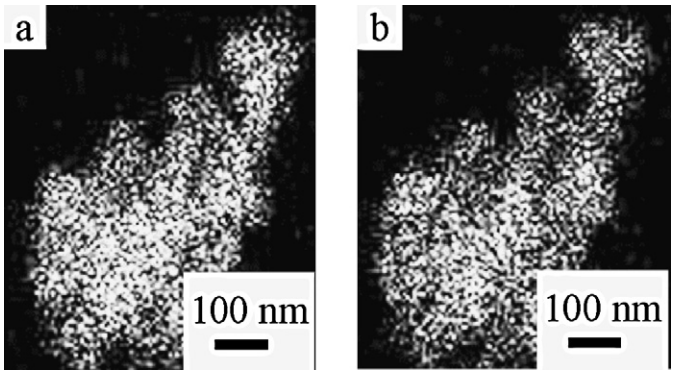

Fig. 3. ESD micrographs of prepared catalyst of $Ni_{0.50}Co_{0.50}$ of (a) Ni component, (b) Co component.

($Ni_{0.75}Co_{0.25}$, $Ni_{0.50}Co_{0.50}$, and $Ni_{0.25}Co_{0.75}$) was analyzed by TEM-EDS, and summarized in Table 1. It well agrees with the starting values used for the preparation. The Ni_xCo_y catalysts were prepared with well-controlled alloy composition using the liquid reduction process without any dispersants.

Fig. 4 shows XPS spectra of Ni 2p and Co 2p region of the prepared catalyst. The metallic Ni at 853 eV and the satellite peaks at 859 eV can be seen in Fig. 4(a). The satellite peak of metallic Ni appears in approximately 6 eV away from Ni 2p3/2 and Ni 2p1/2 toward the high binding energy [11]. The metallic Co at 778 eV and the broad peak of oxidized Co at 781 eV can be seen in Fig. 4(b). The oxidized Co peak strongly appeared comparison with the metallic Co peak on the surface of prepared Ni, $Ni_{0.75}Co_{0.25}$, $Ni_{0.25}Co_{0.75}$, and Co catalyst. However, the metallic Co peak was higher than the oxidized Co peak on the surface of $Ni_{0.50}Co_{0.50}$ catalyst.

Fig. 5 shows the linear sweep voltammetry (LSV) profiles of the prepared Ni, Co, and Ni_xCo_y ($Ni_{0.75}Co_{0.25}$, $Ni_{0.50}Co_{0.50}$, $Ni_{0.25}Co_{0.75}$) catalysts by liquid reduction process from −0.24 V to 0.05 V in 1.0 M KOH/0.1 M $N_2H_4{\cdot}H_2O$ electrolyte solution, and results were summarized in Table 2. The onset potential for each catalyst was −0.21 V for $Ni_{0.50}Co_{0.50}$, −0.16 V for $Ni_{0.75}Co_{0.25}$, −0.14 V for $Ni_{0.25}Co_{0.75}$, −0.09 V for Co, −0.06 V for Ni. The onset potentials for electrooxidation of hydrazine on the NiCo alloy catalysts were lower than the Ni and Co catalysts. This result clearly shows the coexistence effect of Ni and Co in the alloy catalysts prepared by the liquid reduction method. Of course, lower onset potential of $Ni_{0.50}Co_{0.50}$

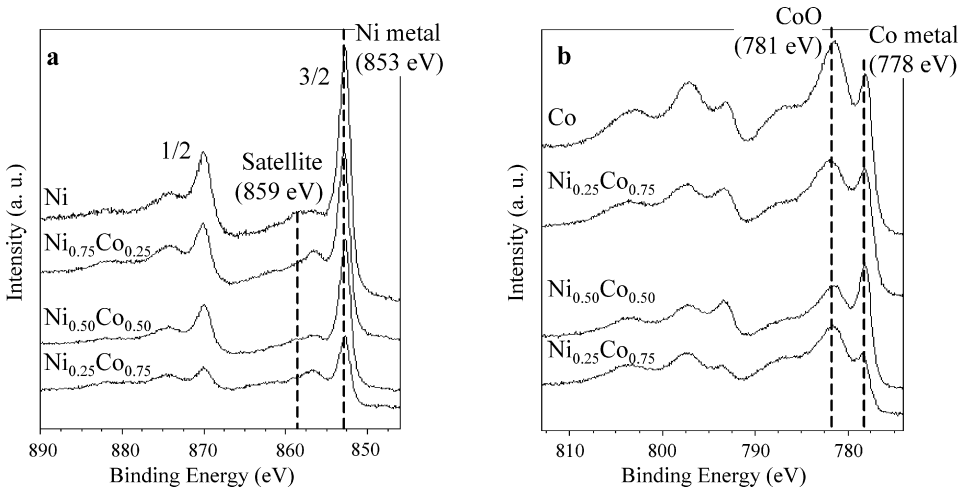

Fig. 4. XPS spectra of prepared catalysts of (a) Ni2p, (b) Co2p region.

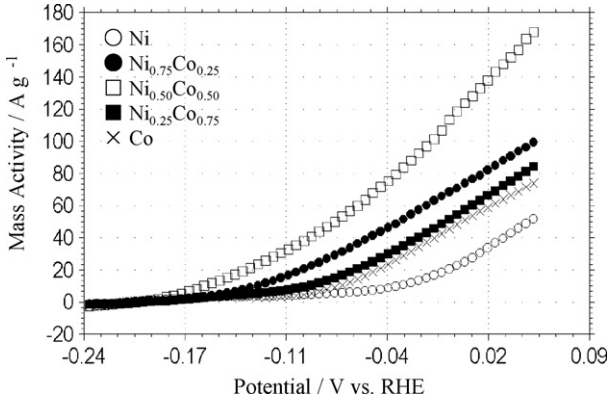

Fig. 5. LSV profiles of prepared catalysts.

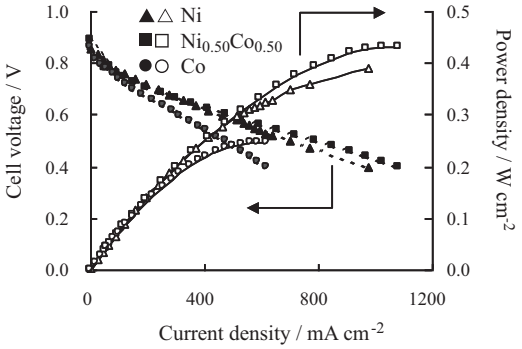

Fig. 6. Cell performance of prepared Ni, $Ni_{0.50}Co_{0.50}$, Co as the anode catalyst of the current–voltage (*I–V*) characteristics and the power density performances (*I–P*). The solid marks are *I–V*, and the frame marks are *I–P* results.

contributes to improve open-circuit voltage (OCV) of PM-fLFCs. The electrooxidation of hydrazine is shown as follows:

$$N_2H_4 + 4OH^- \leftrightarrow N_2 + 4H_2O + 4e^-$$

$$E^\circ = -0.33\,V(\text{vs.RHE, pH} = 14) \quad (1)$$

The overpotential of electrooxidation of hydrazine on the $Ni_{0.50}Co_{0.50}$ catalyst was calculated only 0.12 V from the difference between onset potential and the theoretical potential value of Eq. (1).

The difference of current at 0.05 V in LSV showed that the alloy catalysts have high catalytic activity than Ni and Co. The $Ni_{0.50}Co_{0.50}$ catalyst showed the highest catalytic activity than the other catalysts. The oxidation current is based on electrooxidation of hydrazine, because any current was not observed at same potential region in 1 M KOH electrolyte. Thus it could be concluded that the prepared catalysts were not oxidized themselves. It has been recognized that $Ni_{0.50}Co_{0.50}$ exhibits higher activity by 3.3 and 2.2 times than Ni and Co respectively.

Table 2
Electrical performance of synthesized Ni, Co, and Ni_xCo_y catalysts.

Catalysts	Onset potential (V vs. RHE)	Mass activity (A/cm^2)	OCV (V)	Power density (mW/cm^2)
Ni	−0.06	50.3	0.858	389
$Ni_{0.75}Co_{0.25}$	−0.16	99.8		
$Ni_{0.50}Co_{0.50}$	−0.21	171.2	0.891	432
$Ni_{0.25}Co_{0.75}$	−0.14	82.3		
Co	−0.09	75.0	0.863	246

The cell performance of PM-fLFCs using prepared catalysts as an anode catalyst and Co-PPY-C as a cathode catalyst was summarized in Table 2. The current–voltage (*I–V*) characteristics and the power density performances are shown in Fig. 6. The different *I–V* characteristics in Fig. 6 are observed when using different composition catalysts. The open-circuit voltage (OCV) of PM-fLFCs using $Ni_{0.50}Co_{0.50}$ (0.891 V) is higher than Ni (0.858 V) or Co (0.863 V), which well agrees with RDE results. Moreover, $Ni_{0.50}Co_{0.50}$ ($432\,mW/cm^2$) exhibits a higher power density than Ni ($389\,mW/cm^2$) or Co ($246\,mW/cm^2$). It has been confirmed that the $Ni_{0.50}Co_{0.50}$ synthesized with liquid reduction process contributes to improve cell performance of PM-fLFCs.

4. Conclusions

Ni, Co, Ni_xCo_y ($Ni_{0.75}Co_{0.25}$, $Ni_{0.50}Co_{0.50}$, $Ni_{0.25}Co_{0.75}$) catalysts for the electrooxidation of hydrazine were synthesized using the liquid reduction process, and the Ni_xCo_y alloy compositions were well controlled. TEM-EDS micrographs showed that $Ni_{0.50}Co_{0.50}$ was homogeneously prepared a solid solution of Ni and Co. XPS spectra revealed that the metallic Co peak is higher than the oxidized Co peak on the surface of $Ni_{0.50}Co_{0.50}$ catalyst. The onset potential of $Ni_{0.50}Co_{0.50}$ exhibited −0.21 V that was lower than the other catalysts. The overpotential of electrooxidation of hydrazine on the $Ni_{0.50}Co_{0.50}$ catalyst was calculated only 0.12 V. The prepared catalysts were applied to an anode catalyst of PM-fLFCs, and the cell performance of $Ni_{0.50}Co_{0.50}$ exhibited $432\,mW/cm^2$.

Acknowledgments

Authors thanks to Professor H. Saka and Mr. T. Suzuki (Nagoya University) for the help of TEM observations that was supported by Open Advanced Research Facilities Initiative, High Performance Electron Microscopy in Support of Bio and Nanoscience provided by Ministry of Education, Culture, Sports, Science and Technology (MEXT).

References

[1] G.E. Evans, K.V. Kordesch, Science 158 (1967) 1148.
[2] S. Karp, L. Meites, J. Am. Chem. Soc. 84 (1966) 906.
[3] K. Yamada, K. Yasuda, H. Tanaka, Y. Miyazaki, T. Kobayashi, J. Power Sources 122 (2003) 132.
[4] K. Asazawa, K. Yamada, H. Tanaka, A. Oka, M. Taniguchi, T. Kobayashi, Angew. Chem. Int. Ed. 46 (2007) 8024.
[5] J.R. Varcoe, R.C.T. Slade, Fuel Cells 2 (2005) 187.
[6] J.R. Varcoe, R.C.T. Slade, E.L.H. Yee, Chem. Commun. (2006) 1428.
[7] E.H. Yu, K. Scott, J. Appl. Electrochem. 35 (2005) 91.
[8] K. Yamada, K. Yasuda, N. Fujiwara, Z. Shiroma, H. Tanaka, Y. Miyazaki, T. Kobayashi, Electrochem. Commun. 5 (2003) 892.
[9] J.S. Chinchilla, Z. Liu, K. Asazawa, T. Sakamoto, H. Tanaka, P. Strasser, Abstract 463, Electrochem. Soc. Meeting Abstracts, vol. 2010-1, Vancouver, Canada, April 25–30, 2010.
[10] K. Asazawa, T. Sakamoto, S. Yamaguchi, H. Fujikawa, H. Tanaka, K. Oguro, J. Electrochem. Soc. 156 (2009) B509.
[11] F.U. Hillebrechit, J.C. Fuggle, P.A. Bennett, Z. Zolnierek, Ch. Freiburg, Phys. Rev. B27 (1983) 2180.